A distance meter using a terahertz intermode beat in an optical frequency comb

Shuko Yokoyama[1,2]*, Toshiyuki Yokoyama[2], Yuki Hagihara[1], Tsutomu Araki[1], and Takeshi Yasui[1]

[1]*Graduate School of Engineering Science, Osaka University, 1-3 Machikaneyama, Toyonaka, Osaka 560-8531, Japan*
[2] *Micro-Optics Co. Ltd., 2-26 Oe-Tsukahara, Nishikyoku, Kyoto, 610-1105, Japan*
yokoyama@sml.me.es.osaka-u.ac.jp

Abstract: We propose a distance meter that utilizes an intermode beat of terahertz frequency in an optical frequency comb to perform high resolution and high dynamic range absolute distance measurements. The proposed system is based on a novel method, called *multiheterodyne cross-correlation detection*, in which intermode beat frequencies are scaled down to radio frequencies by optical mixing of two detuned optical frequency combs with a nonlinear optical crystal. Using this method, we obtained a 1.056 THz intermode beat and achieved a distance resolution of 0.820 μm from its phase measurement. Absolute distance measurement using 1.056 THz and 8.187 GHz intermode beats was also demonstrated in the range of 10 mm, resulting in a precision of 0.688 μm.

OCIS codes: (120.0120) Instrumentation, measurement, and metrology; (120.3940) Metrology; (120.5050) Phase measurement; (140.4050) Mode-locked lasers; (280.3400) Laser range finder.

References and links

1. R. Dändliker, R. Thalmann, and D. Prongue, "Two-wavelength laser interferometry using superheterodyne detection," Opt. Lett. **13**(5), 339–341 (1988).
2. S. Yokoyama, J. Ohnishi, S. Iwasaki, K. Seta, H. Matsumoto, and N. Suzuki, "Real-time and high-resolution absolute-distance measurement using an two-wavelength superheterodyne interferometer," Meas. Sci. Technol. **10**(12), 1233–1239 (1999).
3. I. Fujima, S. Iwasaki, and K. Seta, "High-resolution distance meter using optical intensity modulation at 28GHz," Meas. Sci. Technol. **9**(7), 1049–1052 (1998).
4. O. P. Lay, S. Dubovitsky, R. D. Peters, J. P. Burger, S. W. Ahn, W. H. Steier, H. R. Fetterman, and Y. Chang, "MSTAR: a submicrometer absolute metrology system," Opt. Lett. **28**(11), 890–892 (2003).
5. S. T. Cundiff, and J. Ye, "Colloquium: Femtosecond optical frequency combs," Rev. Mod. Phys. **75**(1), 325–342 (2003).
6. J. Ye, "Absolute measurement of a long, arbitrary distance to less than an optical fringe," Opt. Lett. **29**(10), 1153–1155 (2004).
7. I. Coddington, W. C. Swann, L. Nenadovic, and N. R. Newbury, "Rapid and precise absolute distance measurements at long range," Nat. Photonics **3**(6), 351–356 (2009).
8. K. N. Joo, and S. W. Kim, "Absolute distance measurement by dispersive interferometry using a femtosecond pulse laser," Opt. Express **14**(13), 5954–5960 (2006).
9. N. Schuhler, Y. Salvade, S. Leveque, R. Dandliker, and R. Holzwarth, "Frequency-comb-referenced two-wavelength source for absolute distance measurement," Opt. Lett. **31**(21), 3101–3103 (2006).
10. Y. Salvadé, N. Schuhler, S. Lévêque, and S. Le Floch, "High-accuracy absolute distance measurement using frequency comb referenced multiwavelength source," Appl. Opt. **47**(14), 2715–2720 (2008).
11. K. Minoshima, and H. Matsumoto, "High-accuracy measurement of 240-m distance in an optical tunnel by use of a compact femtosecond laser," Appl. Opt. **39**(30), 5512–5517 (2000).
12. K. Minoshima, Y. Sakai, H. Takahashi, H. Inaba, and S. Kawato, "Direct comparison of absolute distance meter using an optical comb and integrated optical interferometer with an optical sub-wavelength accuracy", in *CLEO 2009,* Technical Digest(CD)(Optical Society of America, 2009), paper CTuS6.
13. I. Coddington, W. C. Swann, and N. R. Newbury, "Coherent multiheterodyne spectroscopy using stabilized optical frequency combs," Phys. Rev. Lett. **100**(1), 013902 (2008).
14. A. Schliesser, M. Brehm, F. Keilmann, and D. van der Weide, "Frequency-comb infrared spectrometer for rapid, remote chemical sensing," Opt. Express **13**(22), 9029–9038 (2005).
15. T. Yasui, Y. Kabetani, E. Saneyoshi, S. Yokoyama, and T. Araki, "Terahertz frequency comb by multifrequency-heterodyning photoconductive detection for high-accuracy, high-resolution terahertz spectroscopy," Appl. Phys. Lett. **88**(24), 241104 (2006).

#113549 - $15.00 USD Received 30 Jun 2009; revised 5 Sep 2009; accepted 9 Sep 2009; published 14 Sep 2009

16. D. C. Williams, *Optical methods in engineering metrology* (Chaoman & Hall,1993), Chap.5.
17. A. Yariv, *Optical Electronics in modern communications 5th edition*(Oxford University Press,1997),Chap.8.
18. CASIX, *Crystal guide '99*
19. D. von der Linde, "Characterization of the noise in continuously operating mode-locked lasers," Appl. Phys. B **39**(4), 201–217 (1986).

1. Introduction

High-resolution, high dynamic range distance measurements are required in many areas of science and engineering. Laser interferometry is an established method for measuring distances with a subnanometer resolution; however, it is unable to determine the absolute distance beyond its inherent half-wavelength ambiguity range. To overcome this problem, multiwavelength interferometry has been developed [1,2]. Its range for absolute distance measurements is defined by the synthetic wavelength of multiple lasers; however, the number of synthetic wavelengths that can be used is restricted. On the other hand, a distance meter utilizing sinusoidally intensity-modulated continuous-wave light has been developed for measuring long distances. This method achieves a high resolution by using a high modulation frequency. Studies using frequencies as high as 28 GHz [3] and 40 GHz [4] have been reported.

Recently, optical frequency combs emitted by mode-locked femtosecond lasers have received considerable interest because they are light sources having multiple wavelengths that are coherently related [5]. The optical frequency comb has prompted studies aiming at measuring absolute distance with a high dynamic range by using various methods, including combination of time-of-flight and coherence interferometry [6,7], dispersive interferometry [8], multiwavelength interferometry [9,10], and a modulation method using the intermode beats of the optical frequency comb [11,12].

The intermode beats of all the mode pairs in an optical frequency comb also form a comb structure of optical beats over a wide range that extends from radio frequencies (RF) to terahertz (THz) frequencies; we term this comb structure *an optical beat comb*. An optical beat comb is a collection of accurate and stable modulation frequencies, enabling measurements to be performed over a high dynamic range. Using the optical beat comb, high quality modulation lights are obtained without any external modulator that may introduce cyclic errors in the modulation frequency due to electrical crosstalk. It is well known that distance resolution increases as the modulation frequency of the probe light increases when the measurable phase resolution remains constant. Minoshima et al. have improved the phase resolution of a 40 GHz intermode beat and have performed distance measurements with a resolution of 0.19 μm [12]. In their study, the frequencies in the optical beat comb that could be used were limited to the RF region due to the cut-off frequency of the photodetectors. To achieve a higher resolution, a method is required for detecting optical beats that extends to the THz region.

In frequency-comb spectroscopy, the *multiheterodyne* method has been used to resolve individual lines in the frequency comb in the optical region [13], the infrared region [14], and the THz region [15], by down-converting them to the RF range. If the multiheterodyne method can be modified for frequency-comb-based distance metrology, the frequencies that can be used in an optical beat comb will be greatly increased. We here propose a novel method for obtaining whole intermode beats in an optical beat comb; we call this method *multiheterodyne cross-correlation detection*. In this method, the optical beat comb is scaled down to the RF region by mixing two optical frequency combs that have slightly different spacings using a nonlinear optical crystal. Phase measurement of the THz frequency beat is then performed in the RF region. In experiments, we obtained a 1.056 THz intermode beat and achieved a distance resolution of 0.820 μm. This is the first report of a THz beat being used to measure distance.

Absolute distance measurements using 1.056 THz and 8.187 GHz intermode beats were also demonstrated and high dynamic range distance measurement was confirmed. We found that the resolution depended on the comb mode spacing and thus it should be possible to

#113549 - $15.00 USD Received 30 Jun 2009; revised 5 Sep 2009; accepted 9 Sep 2009; published 14 Sep 2009

achieve much higher resolutions by optimizing the laser source (see discussion in Section 6.2).

2. Principle

2.1 Multiheterodyne cross-correlation detection

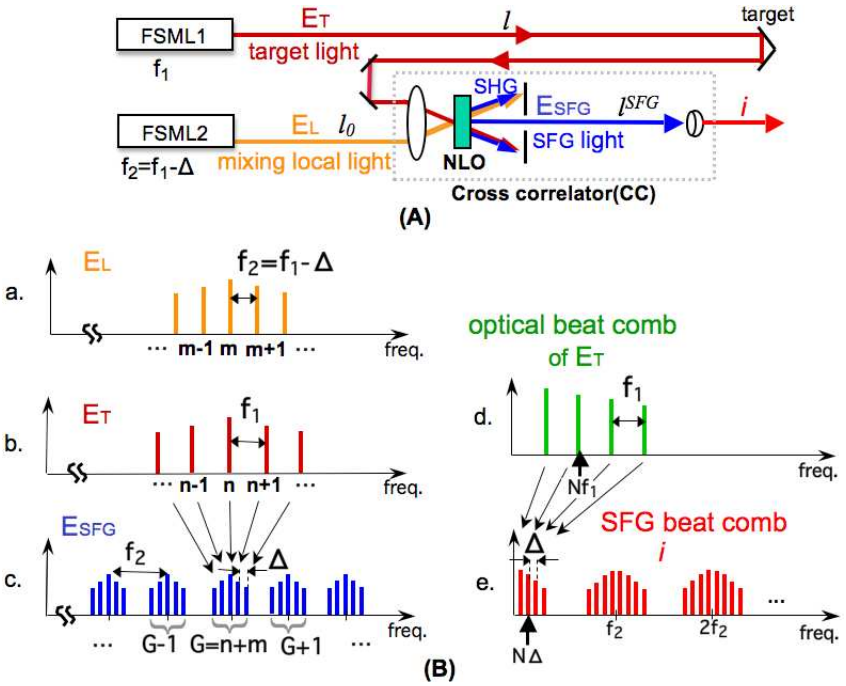

Fig. 1. (A) Optical system and (B) spectral behavior of multiheterodyne cross-correlation detection. FSML: femtosecond mode-locked laser, CC: cross correlator, NLO: nonlinear optical crystal, SHG: second-harmonic generation light and SFG light: sum-frequency generation light.

Figure 1(A) shows the optical system used for *multiheterodyne cross-correlation detection* and Fig. 1(B) shows the spectral behavior of this system. The optical system consists of two femtosecond mode-locked lasers (FSMLs) and a noncollinear cross correlator (CC) for sum-frequency generation (SFG). The CC consists of a focusing lens, a nonlinear optical (NLO) crystal, and a photodetector. The two FSMLs emit two optical-frequency combs, E_T and E_L, where E_T is utilized as the target light and E_L is used as the mixing local light. After illuminating the target, the reflected E_T and E_L lights are focused noncollinearly on the NLO crystal. Here, the mode spacings of E_T and E_L, f_1 and f_2, are set with a small frequency difference Δ (= f_1–f_2) as shown in a and b of Fig. 1(B). Then, E_T and E_L at the NLO crystal are given as:

$$E_T = \sum_n E_{1,n} \cos[2\pi(nf_1 + f_{1o})t + \phi_{1,n}] \quad , \tag{1}$$

$$\phi_{1,n} = -\frac{2\pi(nf_1 + f_{1o})n^p}{c} l \quad , \tag{2}$$

#113549 - $15.00 USD Received 30 Jun 2009; revised 5 Sep 2009; accepted 9 Sep 2009; published 14 Sep 2009

$$E_L = \sum_m E_{2,m} \cos[2\pi(mf_2 + f_{2o})t + \phi_{2,m}] \quad , \tag{3}$$

$$\phi_{2,m} = -\frac{2\pi(mf_2 + f_{2o})n^p}{c} l_0 \quad , \tag{4}$$

where n and m are the mode order, $E_{1,n}$ and $E_{2,m}$ are the field amplitudes of each mode, f_{1o} and f_{2o} are the carrier envelope offset frequencies of E_T and E_L, c is the velocity of light, n^p is the phase refractive index, l and l_0 are the optical path lengths from FSML1 and FSML2 to the NLO crystal, respectively.

When E_T and E_L are focused on the NLO crystal, two second-harmonic generation (SHG) lights and one SFG light of E_T and E_L are generated by the nonlinear optical process. Due to the noncollinear configuration, the two SHG lights and the one SFG light are emitted in different directions, permitting the SFG light to be spatially separated from the SHG lights. The spectrum of the SFG light consists of the sum frequencies of every combination of the E_T and E_L modes due to optical mixing. The field of the SFG light, E_{SFG}, at the detector, which is located a path length l^{SFG} from the NLO crystal, is given by:

$$\begin{aligned} E_{SFG} &\propto \sum_n \sum_m E_{1,n} E_{2,m} \cos[2\pi((n+m)f_2 + n\Delta + f_{1o} + f_{2o})t + \phi_{1,n} + \phi_{2,m} + \theta_{n,m} + \phi_{n,m}^{SFG}] \\ &\equiv \sum_n \sum_m E_{SFG}^{n,m} \end{aligned} \tag{5}$$

$$\phi_{n,m}^{SFG} = -\frac{2\pi((n+m)f_2 + n\Delta + f_{1o} + f_{2o})n_{2\omega}^p}{c} l^{SFG} \quad , \tag{6}$$

where $\theta_{n,m}$ is the phase shift occurring in the mixing process related to the phase mismatch between the fundamental and second harmonics (this is described in detail in Section 6.1) and $n^p{}_{2\omega}$ is the phase refractive index of the second harmonic. Equation (5) shows that the resultant structure of the spectrum of E_{SFG} is divided into mode groups that have the same value of $(n + m) \equiv G$ and that every group has modes separated by Δ (see c in Fig. 1(B)). The mode group of G is generated by mixing the …(n−1), n, (n + 1)… modes of E_T with the …(m + 1), m, (m−1)… modes of E_L, respectively. Note that each mode group of E_{SFG} forms a replica of the E_T spectrum where the mode separation is compressed from f_1 to Δ. This replica preserves the phase information of E_T, $\phi_{1,n}$, which includes the path length l.

When this light is detected by a detector, the spectrum of the output current, i, also forms a comb of beats between each mode in E_{SFG} due to the square law of the detector (see e in Fig. 1(B)), which is called the *SFG beat comb*. In the SFG beat comb, modes generated from the same mode group of E_{SFG} form the lowest group and those generated from adjacent mode groups of E_{SFG} form the second lowest group located at f_2 (see e in Fig. 1(B)). Here, we focus on the lowest group of the SFG beat comb, which is denoted by i_G. As i_G is generated from a pair of modes that have the same value of G (i.e., $E_{SFG}^{n,m}$ and $E_{SFG}^{n+N,m-N}$) it consists of the frequencies $N\Delta$ (N = 1, 2, 3….) as:

#113549 - $15.00 USD Received 30 Jun 2009; revised 5 Sep 2009; accepted 9 Sep 2009; published 14 Sep 2009

$$i_G \propto \sum_{N=1}\{\sum_n \sum_m (E_{SFG}^{n,m} + E_{SFG}^{n+N,m-N})^2\}$$

$$= D.C. + \sum_{N=1}\{\sum_n \sum_m E_{1,n} E_{2,m} E_{1,n+N} E_{2,m-N} \tag{7}$$

$$* \cos[2\pi N\Delta t - \frac{2\pi N f_1 n^g}{c} l + \frac{2\pi N f_2 n^g}{c} l_0 - \frac{2\pi N \Delta n_{2\omega}^g}{c} l^{SFG} + \theta_{n,m} - \theta_{n+N,m-N}]\}$$

where n^g and $n^g{}_{2\omega}$ are the group refractive indices of the fundamental and second-harmonic optical frequencies. The phase is given by the second to sixth terms in the parentheses of the cosine function in Eq. (7); since l relates to the target distance, the second term is the objective phase, and the sum of the third to sixth terms is treated as a constant. The second term, $(2\pi Nf_1 n^g/c)\, l$, is equivalent to the phase variation obtained by beating light of frequency Nf_1 traveling over a path length of l. Thus, the measurement sensitivity using beating light of frequency Nf_1 can be obtained by observing the down-converted frequency of $N\Delta$. The phase of the Nth mode in Eq. (7) is given in terms of l as:

$$\Phi_N = -\frac{2\pi N f_1 n^g}{c} l + \Phi^{ct}{}_N \quad , \tag{8}$$

where $\Phi^{ct}{}_N$ is the constant phase derived from the sum of the third to sixth terms in the parentheses of the cosine function in Eq. (7).

As i_G appears in the lowest band of the SFG beat comb, by setting Δ so that the bandwidth of each mode group of E_{SFG} is less than $f_2/2$, i_G can be separated from the second lowest group of the SFG beat comb (see e in Fig. 1(B)). On the other hand, d in Fig. 1(B) shows the optical beat comb generated from all mode pairs in E_T, assuming that a method for detecting this is available. This comb extends from RF to THz frequencies and has a separation of f_1. Comparing with this, the lowest group of the SFG beat comb, i_G, is regarded as a replica of the optical beat comb, in which the mode separation is compressed from f_1 to Δ. This is because the lowest group of the SFG beat comb is a collection of intermode beats generated within each mode group of E_{SFG} that forms a replica of E_T. The phase corresponding to l measured by frequency Nf_1 can be obtained by selecting the Nth mode in the lowest group of the SFG beat comb.

In the present method, the carrier envelope offset frequencies, f_{1o} and f_{2o}, are canceled in the photodetection process described by Eq. (7), so that they do not influence the objective phase. Therefore, unlike most systems that use two optical-frequency combs, the proposed system does not require stabilization systems for the offset frequencies.

2.2 Absolute distance measurement

The distance of the target from the origin, D, is obtained from the phase Φ_N when $\Phi_N = 0$ at the origin. Then, D can be obtained from the Nth mode frequency:

$$D = \frac{c}{2Nf_1 n_g}\left(I_N + \frac{\Phi_N}{2\pi}\right) \quad , \tag{9}$$

where I_N is the integer fringe order of the Nth mode frequency.

In the absolute distance measurement, two different frequencies are used whose mode orders are defined as N_H and N_L ($N_H > N_L$). The phase is measured using the higher frequency (N_Hth) mode and its fringe order is determined by using the lower frequency (N_Lth) mode. As a result, a distance shorter than half the wavelength of the lower frequency can be measured at the resolution of the higher frequency. The fringe order of the higher frequency, I_{NH}, can then be written in terms of N_H and N_L and the phases of the higher and the lower frequencies, Φ_{NH} and Φ_{NL}, as:

#113549 - $15.00 USD Received 30 Jun 2009; revised 5 Sep 2009; accepted 9 Sep 2009; published 14 Sep 2009

$$I_{NH} = \left[\frac{1}{2\pi} \left(\Phi_{N_L} \frac{N_H}{N_L} - \Phi_{N_H} \right) \right] , \qquad (10)$$

where the square brackets indicate the operation of taking the nearest integer of the argument in Eq. (10). Here, the error in Φ_{NL} must be less than $\pi N_L/N_H$ to correctly determine I_{NH} [2]. Consequently, by using a multiple number of modes in the lowest group of the SFG beat comb, the proposed system can measure absolute distances shorter than half the wavelength of the first mode (frequency = f_1) with a resolution of the higher frequency.

3. Experimental system

Figure 2 shows the configuration of the experimental measurement system used.

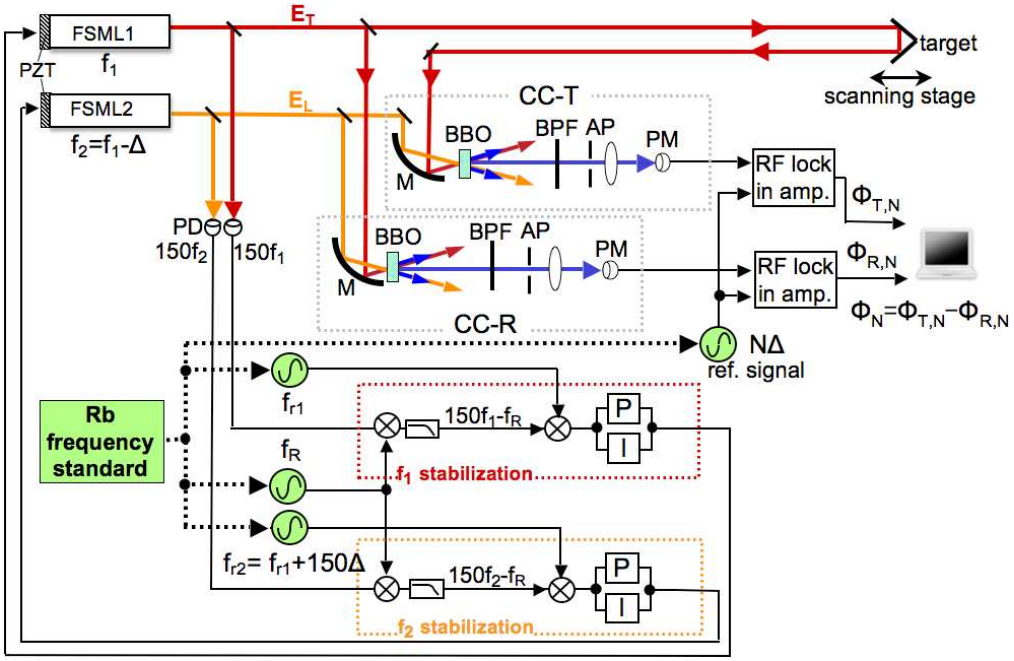

Fig. 2. Experimental setup. PZT: piezoelectric transducer, CC-T and CC-R: cross correlators for target measurement and phase drift compensation, M: parabolic mirror (f = 50 mm), BBO: BBO crystal (type I, 500 μm thick), BPF: blue-pass filter (350–600 nm), AP: aperture, PM: photomultiplier, PD: photodetector and P and I: electrical circuits for proportional and integral control of mode spacing.

A Kerr-lens mode-locked Ti:sapphire laser (FSML: Femtolasers, Femtosource Scientific Pro; total energy = 300 mW, pulse duration = 10 fs, bandwidth = 100 THz, central wavelength = 780 nm) was employed as the FSML. Part of each laser light was split and this light was used to independently stabilize the mode spacing of each laser. Here, the mode spacings of f_1 and f_2 are stabilized at 81.87 MHz with a frequency difference Δ of 650 Hz. Each stabilization system contains a control circuit that includes a double-balanced mixer and a piezoelectric transducer (PZT: Piezomechanik, HPSt150/14; capacitance = 2.6 μF, driver: Thorlabs, MDT694A) attached to the laser cavity mirror. The 150th harmonic components of f_1 and f_2 (12.28 GHz) are down-converted to 10 MHz by mixing with the common reference frequency, f_R (oscillator: Agilent, E8257D). The phases of the resultant frequencies are then locked at the reference frequencies (oscillator: Agilent, 33220A), f_{r1} and f_{r2}, which are set with a difference of 150Δ. Here, all the reference frequencies, f_R, f_{r1}, and f_{r2}, are synchronized to the rubidium frequency standard (Stanford Research Systems, FS725).

#113549 - $15.00 USD Received 30 Jun 2009; revised 5 Sep 2009; accepted 9 Sep 2009; published 14 Sep 2009

The optical system contains two CCs: CC-T and CC-R. CC-T is used to measure the target, while CC-R is used to compensate for phase drift. In both CC-T and CC-R, a parabolic mirror (M; f = 50 mm), a 500-μm-thick BBO crystal (BBO; type I), and a photomultiplier (PM: Hamamatsu, H5783-03; rise time = 0.78 ns) are employed as the focusing lens, the NLO crystal, and the photodetector, respectively. Here, the incident angles of the two lights onto each BBO are ± 5.7° and each BBO was rotated so that the E_T and E_L lights propagate as ordinary lights and the E_{SFG} light propagates as an extraordinary light. A blue-pass filter (BPF; 350–600 nm) was used to select the second-harmonic frequency and an aperture (AP) was used to separate the E_{SFG} light from the two SHG lights.

After splitting the light for stabilizing the mode spacing, both of the E_T and E_L lights are split into two lights and half of the E_T light illuminates the target mirror attached to a precision scanning stage (Suruga Seiki, KS101-20MS; range = 20 mm, reproducibility < ± 0.3 μm, positioning precision < 5 μm), which is located 300 mm from the point where the light is split. After illuminating the target, the reflected E_T light and half of the E_L light are incident on the CC-T. The other E_T and E_L lights are incident on the CC-R. The power of each incident light at the CC is 60–70 mW.

Selection and phase measurement of the Nth mode are performed by two RF digital lock-in amplifiers (Stanford Research Systems, SR844; frequency range = 25 kHz–200 MHz, resolution = 0.02°). Other low-frequency digital lock-in amplifiers (NF, LI5640; frequency range = 1 mHz–100 kHz, resolution = 0.003°) were employed for measuring the phases of signals with frequencies lower than 25 kHz. The time constant was set to 300 ms for all phase measurements. The reference signal of the phase measurement is generated by another oscillator synchronized to the same rubidium frequency standard used for stabilization. From the measured phases of the Nth mode signals obtained from CC-T and CC-R, $\Phi_{T,N}$ and $\Phi_{R,N}$, Φ_N is given by:

$$\Phi_N = \Phi_{T,N} - \Phi_{R,N} \quad . \tag{11}$$

This operation compensates for phase drift. It enables the phase drifts to be compensated that arise in both $\Phi_{T,N}$ and $\Phi_{R,N}$ in the same manner (such as drift in the control circuits of the stabilization system and frequency drift of the reference signal used for the phase measurements). The phase shift obtained by scanning the stage was measured to evaluate the measurement system. An origin is necessary to determine the absolute distance of the target. However, an origin was not set up in this experimental system; instead, the initial position of the scanning stage was taken to be the origin and Φ_N was initialized there.

To evaluate the instabilities in f_1, f_2, and Δ, we measured the repetition frequencies of pulse trains emitted from the two lasers and the cross-correlation signal of the two laser lights, which is produced at the CC, using an RF counter (Agilent, 53132A). Figure 3 shows the resultant instabilities in f_1, f_2, and Δ in terms of the standard deviation as a function of the gate time from 1 ms to 100 s. The instability of the rubidium (Rb) frequency standard, which is also evaluated by the standard deviation, is also shown for comparison. This figure indicates that the instability in Δ is of the order of 10^{-8} (τ = 1 s) and that the instabilities in f_1 and f_2 are the same order of that of the Rb frequency standard. The instabilities in f_1 and f_2 at the gate time of 10 s are better than that in the Rb frequency standard; this is considered caused by measurement error arising from the experiment conditions because f_1 and f_2 are stabilized referring to the Rb frequency standard and their instabilities should not exceed that in the Rb frequency standard.

#113549 - $15.00 USD Received 30 Jun 2009; revised 5 Sep 2009; accepted 9 Sep 2009; published 14 Sep 2009

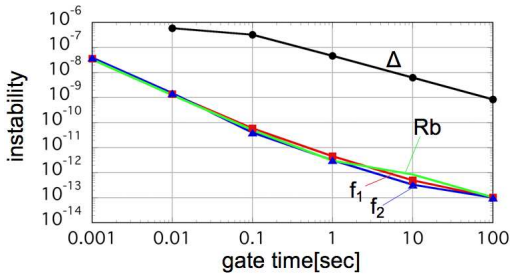

Fig. 3. Instabilities of f_1, f_2, Δ, and the rubidium frequency standard evaluated by the standard deviation with respect to the gate time.

4. Observation of a terahertz mode in the optical beat comb

4.1 Observation of an optical beat comb by a SFG beat comb

First, we investigated the optical beat comb spectrum observed by the SFG beat comb using an RF spectrum analyzer (Agilent, E4402B). Figure 4 shows typical optical beat comb modes in different frequency regions. The background noise, which includes detector and instrument noise, is also shown by the gray line. In each figure, three comb modes were observed with a separation of 81.87 MHz and a continuous spectrum between them. As shown in Fig. 4c, a comb mode with a frequency of 1.056 THz was clearly observed. In Fig. 4d, a comb mode of 2.047 THz is also visible, but its height is only slightly higher than the surrounding continuous spectrum.

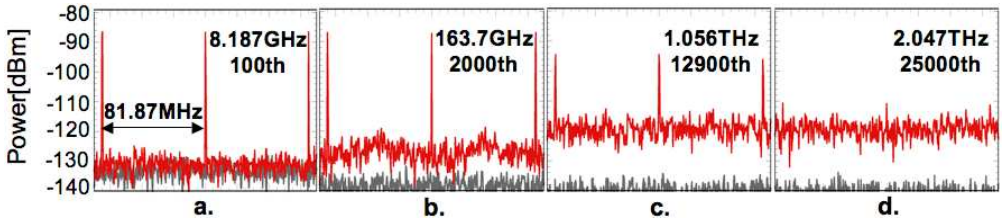

Fig. 4. Typical optical beat comb modes in different frequency regions observed by the SFG beat comb modes (red: comb modes, gray: background noise). Spectrum analyzer settings: resolution bandwidth = 1 Hz, sweep time = 4.6 s, span = 1.4 kHz.

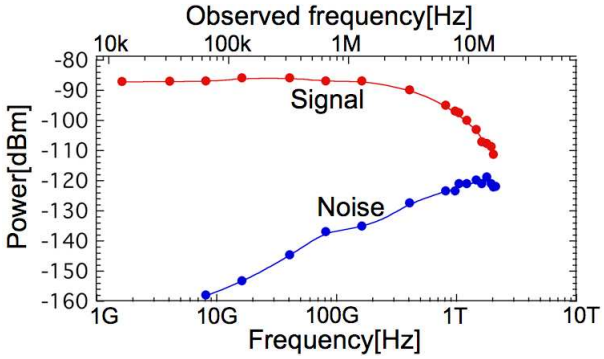

Fig. 5. Power of signal and noise calculated from the optical beat spectrum in Fig. 4. The signal indicates the comb mode level and the noise is the average level of the continuous spectrum between comb modes. The background noise, which includes detector and instrument noise, was subtracted. The upper scale indicates the observed frequency of the SFG beat comb when Δ is 650 Hz and the lower scale indicates the optical beat comb frequency.

Figure 5 shows the signal and noise levels calculated from the optical beat spectra. Here, the signal is the peak power level of the comb mode and the noise is the average level of the

#113549 - $15.00 USD Received 30 Jun 2009; revised 5 Sep 2009; accepted 9 Sep 2009; published 14 Sep 2009

continuous spectrum between comb modes. The background noise was subtracted from the observed level. The upper scale indicates the observed frequency of the SFG beat comb when Δ is 650 Hz, while the lower scale indicates the frequency of the optical beat comb. In this figure, the signal remains constant up to a frequency of about 200 GHz. It then decreases gradually as the frequency increases from 200 GHz to 2.047 THz. A signal was not observed at 2.129 THz. By contrast, the noise is lower than the detectable level at frequencies less than 8 GHz and it increases monotonically above this frequency. One reason why the signal decreases above 200 GHz is considered to be the reduction in the number of mode pairs that generate the SFG beat comb mode. On the other hand, the increase of the noise is considered to reflect the fluctuations in the mode spacing. We discuss the structure of the noise and then explain the experimental results based on it in Section 6.2.

Next, we investigated the dependence of the signal and noise levels on the value of Δ (i.e., the mode spacing of the SFG beat comb) to determine the optimum value of Δ. The signal, noise, and phase fluctuations at 1.056 THz were measured for various values of Δ. The standard deviation of Φ_N measured over a period of 125 s was adopted as the phase fluctuation. Figure 6(a) shows the signal and noise levels for various values of Δ. It shows that the signal level remains almost constant, whereas the noise decreases monotonically with an increase in Δ up to 700 Hz. We calculated the signal-to-noise ratio (SNR) from Fig. 6(a). The resulting SNR is shown in Fig. 6(b) together with the phase fluctuation. This figure shows that the phase fluctuation decreases when the SNR increases and that the phase fluctuation has a minimum value at Δ = 650 Hz in the present experimental setup. Therefore, we set Δ to 650 Hz in all the other measurements performed in this study.

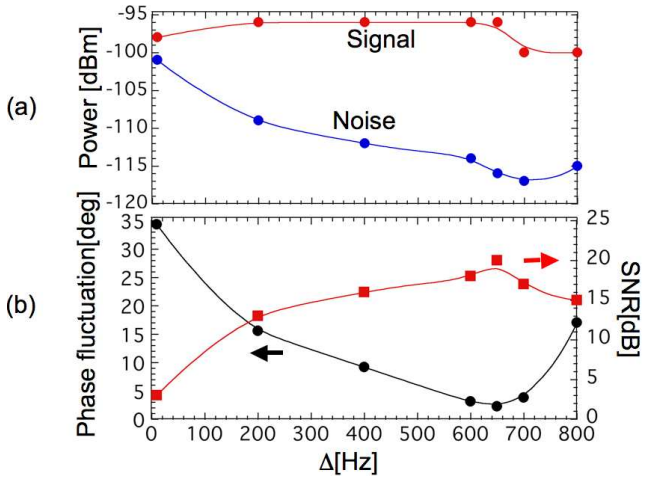

Fig. 6. (a) Power of signal and noise and (b) phase fluctuation and signal-to-noise ratio (SNR) of 1.056 THz with respect to Δ. Phase fluctuation was the standard deviation over a 125 s measurement with a time constant of 300 ms and the SNR was calculated from (a).

Finally, we measured the phase for various frequencies of the optical beat comb. Figure 7 shows the phase fluctuation and the SNR calculated from Fig. 5. This figure also shows the obvious relationship between the phase fluctuation and the SNR. The fluctuation is small at low frequencies where the noise is under the detectable level and it gradually increases with the reduction in the SNR before increasing rapidly just before 2 THz, where the SNR is less than 20 dB. Here, the SNR of the 1.056 THz comb mode is 23 dB and the phase fluctuation is 2.08°, which corresponds to a distance of 0.820 μm. These results demonstrate that the 1.056 THz beat can be used to measure distance with a submicrometer resolution.

#113549 - $15.00 USD Received 30 Jun 2009; revised 5 Sep 2009; accepted 9 Sep 2009; published 14 Sep 2009

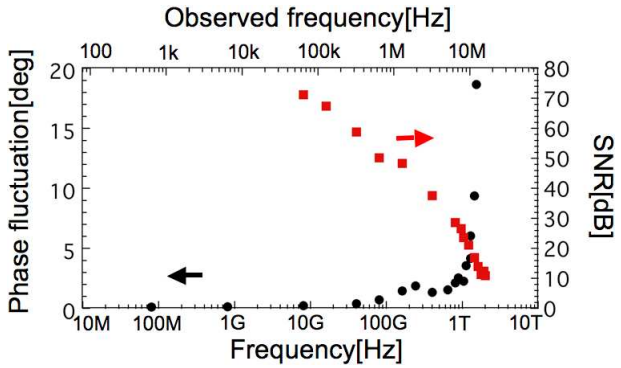

Fig. 7. Phase fluctuation and signal-to-noise ratio (SNR) of optical beat comb. The upper scale indicates the observed frequency of SFG beat comb when Δ is 650 Hz and the lower scale indicates the frequency of the optical beat comb. The phase fluctuation is the standard deviation over a 125 s measurement with a time constant of 300 ms and the SNR is calculated from Fig. 5.

4.2 Distance measurement using the 1.056 THz beat

We performed distance measurements using the 1.056 THz (λ = 284 μm) beat to confirm that the corresponding SFG beat preserves the phase information of the mode of the optical beat comb. The 1.056 THz beat is the 12,900th mode in the optical beat comb and it corresponds to the 8.385 MHz beat in the SFG beat comb.

The stage was moved in 10 μm steps over a total distance of 150 μm, which is approximately half the wavelength of the 1.056 THz beat. The phase Φ_N was measured at each 10 μm step and its value was averaged over a period of 15 s and used to determine the displacement. This scanning over 150 μm was executed sequentially five times. Φ_N was initialized to zero once for all measurements at the initial position of the first scan. The total measurement time was 40 min. The distance of the target from the initial position, D, can be calculated from Eq. (9), where N = 12,900, $I_N = 0$, $f_1 = 81.87$ MHz, and $n^g = 1.000277$ (using Edlen's formula [16] with a temperature of 18°C and a pressure of 1013.25 mbar). Figure 8(a) shows that the calculated distance values plotted as a function of the stage displacement (determined from the number of pulses used to drive the stage). Figure 8(a) also shows the linear approximation, which is given by D = 1.005X − 0.3598. This relationship between the stage scale and the measured distance confirms that the phase information of the 1.056 THz mode in the optical beat comb can be successfully obtained by the present method. However, more precise evaluation by comparing with interferometric measurements is required to confirm the accuracy of this method.

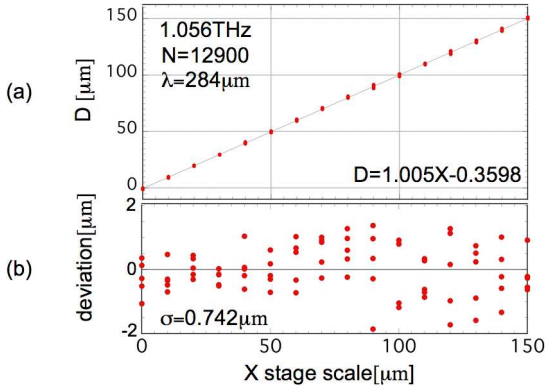

Fig. 8. Distance measurement using the 1.056 THz mode. (a) Measured distance with respect to the stage scale and linear approximation. (b) Deviations from the linear approximation.

#113549 - $15.00 USD Received 30 Jun 2009; revised 5 Sep 2009; accepted 9 Sep 2009; published 14 Sep 2009

The deviation of each data point from this line is depicted in Fig. 8(b). The standard deviation of the error is 0.742 μm. This result suggests that a submicrometer precision can be attained utilizing the 1.056 THz mode.

5. Absolute distance measurement using 1.056 THz and 8.187 GHz

Absolute distance measurement can be realized using multiple modes in the optical beat comb, as described in Section 2.2. We demonstrate that absolute distance measurements can be performed using the 8.17 GHz mode (λ = 36720 μm) in conjunction with the 1.056 THz mode for determining the fringe order, I_{NH} (see Eq. (10)). The mode orders of the 1.056 THz and 8.187 GHz modes, N_H and N_L, are 12,900 and 100, respectively. The spectrum of the 8.187 GHz mode is shown in Fig. 4a. The measured SNR is 70 dB and the phase fluctuation is 0.16° (corresponding to a distance resolution of 8.16 μm), which is sufficiently small to determine I_{NH}.

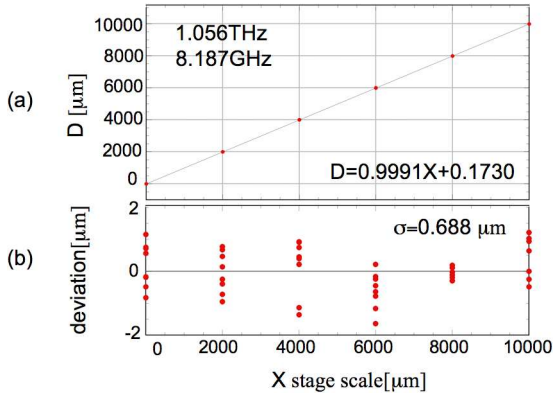

Fig. 9. Absolute distance measurement using the 1.056 THz mode (λ = 284 μm, N = 12,900) and the 8.187 GHz mode (λ = 36,720 μm, N = 100). (a) Measured distance with respect to the stage scale and linear approximation. (b) Deviations from the linear approximation.

The stage was moved in 2 mm steps over a total distance of 10 mm. This scan over 10 mm was executed sequentially eight times. Φ_N was initialized to zero at the initial position of the first scan. The total measurement time was 50 min. The phases of the 8.187 GHz and 1.056 THz modes, Φ_{NL} and Φ_{NH}, were measured sequentially at each step. I_{NH} was calculated using Eq. (10) and the target distance from the initial position was obtained using Eq. (9). The results are plotted as a function of the stage displacement in Fig. 9(a), which also shows the linear approximation (D = 0.9991X + 0.1730). The deviation of each measured value from this line is depicted in Fig. 9(b). The standard deviation of the error was 0.688 μm. This demonstrates that the 1.056 THz and 8.187 GHz modes can be used to measure the absolute distance with a submicrometer precision over a distance of 10 mm.

Adding the first optical beat mode of the 81.87 MHz mode (λ = 3,662 mm) to the 1.056 THz and 8.187 GHz modes extends the absolute distance that can be measured with this system to 1836 mm with a precision defined by the 1.056 THz mode.

In the present measurements, the error in the distance includes 1) positioning error mainly caused by insufficient precision of the screw pitch of the stage, 2) alignment error between the direction of the stage movement and the target light (i.e., a cosine error), and 3) variations in the optical path length caused by temperature and atmospheric pressure fluctuations over the measurement time, in addition to the systematic error of this method. Currently, the stage scale is not sufficiently accurate to evaluate these errors. In the future, we intend to evaluate the system performance in detail by using an interferometer as a reference.

#113549 - $15.00 USD Received 30 Jun 2009; revised 5 Sep 2009; accepted 9 Sep 2009; published 14 Sep 2009

6. Discussion

6.1 Phase shift of the SFG light in the NLO crystal

Here, we discuss the phase shift of the SFG light that occurs in the mixing process in the NLO crystal (defined as $\theta_{n,m}$ in Eq. (5)). We give the derivation of this phase shift and then discuss its variation with the operating conditions of the NLO crystal, such as the temperature and the incident angle of the light.

In the case of a frequency comb, the phase-matching condition between the fundamental and second-harmonic frequencies is not simultaneously satisfied for all frequencies over the comb bandwidth; thus, the phase shift term $\theta_{n,m}$ should generally be included. When the phase-matching condition between the fundamental and the second-harmonic frequencies is not satisfied, the phase shift in the NLO crystal is a function of the wave vector mismatch [17]. $\theta_{n,m}$ is defined as:

$$\theta_{n,m} = \tan^{-1}\left(\frac{\sin\left(\Delta\mathbf{k}_{n,m}\bullet\mathbf{L}\right)}{\cos\left(\Delta\mathbf{k}_{n,m}\bullet\mathbf{L}\right)-1}\right) - \theta_0 \tag{12}$$

$$\theta_0 = 0^\circ\ (\Delta\mathbf{k}_{n,m}\bullet\mathbf{L} > 0),\quad \theta_0 = 180^\circ\ (\Delta\mathbf{k}_{n,m}\bullet\mathbf{L} < 0)\quad ,$$

$$\Delta k_{n,m} = k_n + k_m - k_{n,m,} \tag{13}$$

where $\Delta\mathbf{k}_{n,m}$ is the wave vector mismatch, and $\mathbf{k}_n$, $\mathbf{k}_m$, and $\mathbf{k}_{n,m}$ are the wave vectors of E_T, E_L, and E_{SFG}, respectively. **L** is the length vector of the NLO crystal, whose direction is normal to the NLO crystal. When $\Delta\mathbf{k}_{n,m}\bullet\mathbf{L} = M*360^\circ$ ($M = \pm 1, \pm 2,\ldots$), $\theta_{n,m}$ is indefinite. However, in this condition, the amplitude becomes zero (i.e., the corresponding mode does not exist).

When the temperature or the incident angle of the light in the NLO crystal changes during the measurement, $\theta_{n,m}$ varies causing a variation in the phase of SFG beat, $\theta_{n,m}-\theta_{n+N,m-N}$ (see Eq. (7)), which gives rise to a measurement error. We estimated the amount of variation in $\theta_{n,m}-\theta_{n+N,m-N}$. When the refractive indices of ordinary light (E_T and E_L) and extraordinary light (E_{SFG}) in the NLO crystal, n_o and n_e^{φ}, vary with temperature, $\Delta\mathbf{k}_{n,m}$ also varies because $\mathbf{k}_n$, $\mathbf{k}_m$, and $\mathbf{k}_{n,m}$ depend on these indices. The following assumptions are made in the estimation: the center frequency and the bandwidth of the E_T and E_L lights are 384 THz (780 nm) and 100 THz, respectively; the incident angle of the E_T and E_L lights at the NLO crystal are ± 5.7°; the NLO crystal is BBO; this crystal is cut so that the angle of the crystal-surface-normal to the optical axis is 29.9° (the phase matching angle for the 384 THz); and L is 500 μm. The refractive indices of the principal axes of the crystal, n_o and n_e, are dependent on the frequency and they are calculated using the Sellmeier equation, and the thermo-optic coefficients of n_o and n_e, dn_o/dT and dn_e/dT are -9.3×10^{-6}/°C and -16.6×10^{-6}/°C, respectively [18]. The variation of $\theta_{n,m}-\theta_{n+N,m-N}$ for a temperature change of 1°C was calculated to be approximately 0.0004° for the 1 THz SFG beat, which corresponds to a distance of 0.00016 μm.

On the other hand, we assume that one of the incident lights to the NLO crystal changes its incident angle by 0.1°, which occurs when the target light is shifted by 100 μm by vertical movement of the corner reflector. Based on this estimation, the variation in $\theta_{n,m}-\theta_{n+N,m-N}$ of the 1 THz SFG beat is approximately 0.06°, which corresponds to a distance of 0.02 μm. Although the incident angle also changes when the direction of the laser beam changes, it gives rise to a more significant error in the distance measurement than the phase error in the NLO. These estimations reveal that the phase variation caused by temperature change is negligibly small. However, the phase is more sensitive to variations in the incident angle; thus, a rigid mechanical setup is required in addition to adequate pointing stability of the laser beams. We will take these errors into account when improving the measurement precision.

#113549 - $15.00 USD Received 30 Jun 2009; revised 5 Sep 2009; accepted 9 Sep 2009; published 14 Sep 2009

6.2 Noise structure and improvement of the distance resolution

In the present experiment, a submicrometer resolution was achieved using the 1.056 THz optical beat. It is obvious from experimental results in Section 4.1 that to further enhance the distance resolution the SNR needs to be improved either to suppress the phase fluctuations of the SFG beat or to enable higher-order modes to be utilized. Here, we discuss the structure of the noise and some countermeasures for improving the SNR based on a knowledge of the noise structure.

A pulse train emitted by a mode-locked laser generally contains fluctuations in amplitude and repetition frequency. These fluctuations form a pedestal at each δ-function-like mode in the intermode beat comb and the fluctuation in repetition frequency causes the area of pedestal to increase as the mode order increases [19].

The SFG light also forms a pulse train that has fluctuations in amplitude and repetition frequency. It is inferred that a pedestal is formed at each mode in the SFG beat comb and becomes larger with the mode order. Because the mode spacing of the SFG beat comb, Δ, is small compared with the optical beat comb, it is considered that pedestals of multiple adjacent modes are accumulate and form a continuous spectrum between the SFG beat comb modes, as observed in Fig. 4. The increase in the area of each pedestal with the mode order well explains the experimental results in Fig. 5 that show that the noise increases monotonically with frequency. The experimental results in Fig. 6(a) show that the noise level is approximately inversely proportional to Δ. This is because the number of pedestals that accumulate between adjacent modes decreases when Δ increases.

On the other hand, the SFG beat comb consists of many groups (see e of Fig. 1(B)). When Δ is too large, the second lowest group may overlap with the lowest group, increasing the noise level of the higher frequency region of the lowest group of the SFG beat comb. This might explain the experimental results in Fig. 6(a), which show that the noise level no longer decreases when Δ is greater than 700 Hz.

The area of the pedestal in each SFG beat comb mode depends on the instabilities of f_1, f_2, and Δ, as described above. In the present experiment, the instability in the gate time of less than 1 ms might be insufficient, because the bandwidth of the feedback control in the stabilization system is limited to 400 Hz by the capacitance of the PZT (2.6 μF). Thus, using a PZT with a lower capacitance would improve the instability for short gate times. As a result, the noise is expected to decrease.

From the above discussion, a larger Δ is required to obtain a high SNR; however, the mode spacing of the optical frequency comb, f_2, should be large enough to avoid the lowest and second-lowest groups of the SFG beat comb overlapping. Accordingly, to improve the distance resolution, 1) large mode spacings in f_1, f_2, and Δ and 2) high stabilities of these values are necessary.

With the present setup, we confirmed that a terahertz beat obtained using the proposed method can be used for submicrometer precision measurements using a Ti:sapphire laser. In the future, we intend to employ a mode-locked erbium-doped fiber laser as the light source, because its robustness, compactness, and cost-effectiveness make it suitable for use in practical applications. Furthermore, using a fiber laser has the advantages of a high stability of mode spacing and stable beam pointing because fiber lasers do not employ a free-space cavity but rather a fiber cavity, which is tolerant of disturbances in the surrounding environment. We plan to employ fiber lasers with larger mode spacings and to optimize the frequency difference between them, with the goal of obtaining higher-order SFG beat comb modes and achieving a higher resolution.

7. Conclusion

A distance meter utilizing a THz frequency intermode beat of an optical frequency comb has been proposed for absolute distance measurements with a high resolution and a high dynamic range. The proposed system is based on multiheterodyne cross-correlation detection in which intermode beats are down-converted to the RF region. With this method, 1.056 THz

#113549 - $15.00 USD Received 30 Jun 2009; revised 5 Sep 2009; accepted 9 Sep 2009; published 14 Sep 2009

intermode beat was obtained and a submicrometer distance resolution of 0.820 μm was achieved. Absolute distance measurement using the 1.056 THz and 8.187 GHz intermode beats was also demonstrated. In the future, we intend to improve the measurement precision by introducing fiber lasers, which have optimal mode spacing, and to evaluate the resultant accuracy using an interferometer.

Acknowledgements

The authors are grateful to Dr. Kaoru Minoshima of the National Institute of Advanced Industrial Science and Technology, Japan, for helpful discussions and comments and Prof. Tetsuo Iwata of the University of Tokushima for supplying the experimental equipment. This work was supported by a Grant-in-Aid for Scientific Research by the Ministry of Education, Culture, Sports, Science and Technology of Japan (No. 20560036), and the Mitsutoyo Association for Science and Technology Foundation.

#113549 - $15.00 USD Received 30 Jun 2009; revised 5 Sep 2009; accepted 9 Sep 2009; published 14 Sep 2009